Reliability Testing of Free Space Optical Systems in Laboratory Conditions

Tsvetan Mitsev[1], Kalin Dimitrov[2] , Nikolay Kolev[3]

Abstract – **This paper deals with principle schemes of transmitter and receiver of a Free Space Optic (FSO) system and the organisation of experiments with it. We have shown measurements for the verification of its working ability. We have made comparisons with theoretical results.**

Keywords – Free Space Optical Systems, Experimental Setup, Reliability Testing.

I. INTRODUCTION

In the literature there are many theoretical results from research on the working reliability of FSO systems [1-6]. Most papers usually deal with the dependence of FSO on the length of the communication channel, the working wavelength [7,8] and the concrete meteorological conditions [9]. The losses caused by the atmosphere are usually expressed by the visibility S_M [3,10]. Some papers also discuss the fluctuations in the direction of laser ray propagation, caused by other various non-atmospheric factors (building sway [11]).

According to the authors, the experimental verifications and checks of these results present in the literature are very scarce. Probably the reason is basically the labour consumption during the setting up of such experiments, the impossibility for some of the parameters of the experiment to be easily changed or even predicted. We have to add to the abovementioned facts the necessary long overall time duration of possible complex research.

These reasons have resulted in the setting up of a laboratory setup with a controlled simulation of conditions maximally close to the real working ones, for a research on the working reliability of FSO systems depending on the characteristics of their transmitter and receiver systems and also on the parameter of the atmospheric channel.

II. THEORETICAL BACKGROUND

Before we discuss the practical research, we will derive the theoretical expressions necessary for the comparison.

We will start by discussing a laser source [10,12,13]. During a Gaussian amplitude distribution of the light intensity in the transmitting aperture, the intensity at point (ρ, z), in a cylindrical coordinate system and during assumption of azimuthal symmetry, is shown [4] by the expression

$$I(\rho,z) = I_m \frac{\rho_0^2}{\rho_z^2(z)} \exp\left(-2\frac{\rho^2}{\rho_z^2(z)}\right)\tau_a(z) \quad , \qquad (1)$$

where

$$I_m = \frac{2\Phi_L}{\pi\rho_0^2\left(1-e^{-2}\right)} \qquad (2)$$

is the intensity of the light radiation in the centre of the transmitting aperture (maximal intensity), when the power of the source of optical radiation is Φ_L and the losses in the transmitter optics are not taken into account, and ρ_0 is the radius of the Gaussian laser beam in the transmitting aperture (that is, when $z = 0$). The radius of the Gaussian laser beam at a distance z when the wavelength of the optical radiation λ is defined by

$$\rho_z(z) = \frac{\lambda}{\pi\rho_0} z \, . \qquad (3)$$

The expression (3) is valid when the condition $z \geq 10\left(\rho_0^2/\lambda\right)$ is fulfilled. To measure the losses during the propagation of the optical radiation through the communication channel we will use the quantity transmittance

$$\tau_a(z) = \exp\left(-0{,}23.b_f[dB/km].z[km]\right), \qquad (4)$$

where $z \in [0, z]$, and b_f are the distributed losses of the channel. For the atmosphere Eq. (4) is defined by the extinction coefficient

$$b_f[dB/km] = 4{,}343.\alpha_e[km^{-1}] \, . \qquad (5)$$

To define a concrete numerical value Eq. (5) we usually use the half-empirical relation with the meteorological distance of visibility

$$\alpha_e[km^{-1}] = \frac{3{,}92}{S_M[km]}\left(\frac{\lambda[\mu m]}{0{,}55}\right)^{-0{,}585\sqrt[3]{S_M[km]}} \, . \qquad (6)$$

It is evident from expressions (1) and (2) that the change in the intensity of the optical radiation in the point (ρ, z) with constant transmitter parameters is due to two factors: lowering

[1] Tsvetan Mitsev is with the Faculty of Telecommunications at Technical University Technical University of Sofia, 8 Kl. Ohridski Blvd, Sofia 1000, Bulgaria, E-mail: mitzev@tu-sofia.bg.

[2] Kalin Dimitrov is with the Faculty of Telecommunications at Technical University of Sofia, 8 Kl. Ohridski Blvd, Sofia 1000, Bulgaria, E-mail: kld@tu-sofia.bg.

[3]Nikolay Kolev is with the Faculty of Telecommunications at Technical University Technical University of Sofia, 8 Kl. Ohridski Blvd, Sofia 1000, Bulgaria

of the intensity $I(0,z)$ along the axis of the ray due to its divergence and the losses in the transmission channel.

If the radius of the transmitter aperture R_r meets the condition $R_r << \rho_z << z$, then the power $\Phi_{r,s}$ coming form the transmitter into the receiver, when the losses are not taken into account, is

$$\Phi_{r,s} = \pi R_r^2 I(\rho,z). \quad (7)$$

During background radiation with receiver power $\Phi_{r,B}$ the total received power can be calculated by the formula

$$\Phi_r = \Phi_{r,s} + \Phi_{r,B}. \quad (8)$$

We substitute in Eq. (8) the expressions (1), (4), (5), (6) and (7) and we derive

$$\Phi_r = 10\lg\left\{\frac{2}{1-e^{-2}}\cdot\left(\frac{R_r}{\theta_t z}\right)^2 .10^{\frac{\Phi_L}{10}} \times \right.$$
$$\left. \times \exp\left[-2\left(\frac{\theta}{\theta_t}\right)^2 - 2{,}3.10^{-4}.b_f.z\right] + 10^{\frac{\Phi_{r,B}}{10}}\right\}, \quad (9)$$

where θ_t is the angle divergence of the ray after the transmitter aperture, and θ is the angle displacement of the axis of the laser ray according to the direction of the receiver aperture centre. The powers participating in the equation are in [dBm], the angles in [rad], and the distributed losses in [dB/km].

When there are very low values of the background optical flux $\Phi_{r,B}$ and very low distributed losses along the transmission channel Eq. (9) is defined by

$$\Phi_r[dBm] =$$
$$= \Phi_L[dBm] + 20.\lg\left(\frac{R_r}{\theta_t z}\right) - 8{,}686.\left(\frac{\theta}{\theta_t}\right)^2 + 3{,}642 . \quad (10)$$

III. Experimental Setup

The structural scheme of the laboratory test-bed is displayed on Fig. 1.

On the immobile rail (Fig.1, pos.1) we have placed the transmitter (Fig.1, pos.2) and the receiver (Fig.1, pos.3). The distance L between them meets the condition according to which the receiver has to be in the Fresnel zone, and in separate cases only in the Fresnel zone.

The transmitter has been placed on a horizontally rotating (by azimuth) stage (Fig.1, pos.4). With a view to the possibility of a fine adjustment, the receiver has been placed on a x-y-z stage {3D} (Fig.1, pos.5) and it can also be rotated by azimuth. The elevation angle of both blocks is constant and it equals 0. The distribution of the optical radiation of the source in a plane which is cross to the distribution is synphase

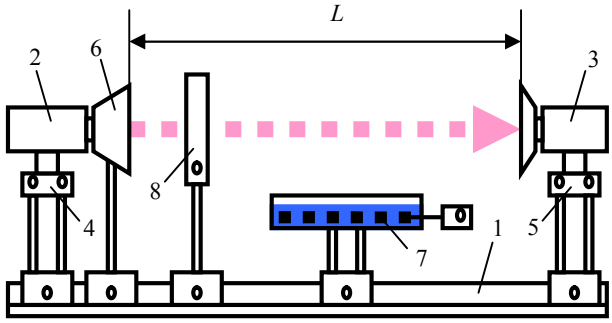

Fig. 1. Laboratory test-bed

and Gaussian amplitude. By means of a readjustable two lens collimator, Kepler's type (Fig.1, pos.6), the necessary beam changes are provided for the simulations of real conditions. For the fixed distance $z = const$ the Gaussian amplitude distribution is preserved, but the current beam radius of $\rho_z(z)$ changes, which equals a change in the divergence of the beam θ_t.

The increasing of θ_t brings about a change in the character of the interaction between the laser radiation and the heterogenities in the field of distribution. At a short distance there is a simulation of an influence over the distribution of the radiation of random heterogenities, turbulence vortices, with larger sizes, which is characteristic of longer real fields.

The collimator makes possible the change of θ_t within wide limits – $\theta_t \in [1mrad; 0{,}3rad]$.

The vaporizer (Fig.1, pos.7) is used for the creation of a randomly heterogeneity medium in the connection channel, which stimulates thoroughly the real turbulence heterogenities during the distribution of the optical radiation in the atmosphere. Its characteristics can change by means of altering the working intensity of the vaporizer. The level of turbulence or vortices distribution along the field changes by means of a fan speed.

The change of the attenuation along the connection channel resulting from the alterations in its transparency, that is the integral changes of the volume extinction coefficient α_e, respectively the meteorological visibility distance S_M, is simulated by placing neutral filters along the laser radiation distribution field. (Fig.1, pos.8). Their location is in conformity with the condition according to which they must not influence the value of the background radiation during the measurements. The filters used have band pass values within the interval $\tau_F \in [0{,}4; 0{,}97]$, which provide values of the simulated meteorological visibility distance along the connection channel within the interval $S_M \in [5{,}5km; 60km]$.

In order to avoid an unnecessary drain of money and time, the electronic blocks of the system have also been programme-tested as early as the design stage, before their physical implementation [14].

The structural scheme of the electronic blocks of the measurement test-bed for BER in Fig.1 consists of a transmitter TX, receiver RX (Fig. 2).

The transmitter TX has 3 outputs – B1, B2 and SYNC. Signals are transmitted to the receiver, which are subject to

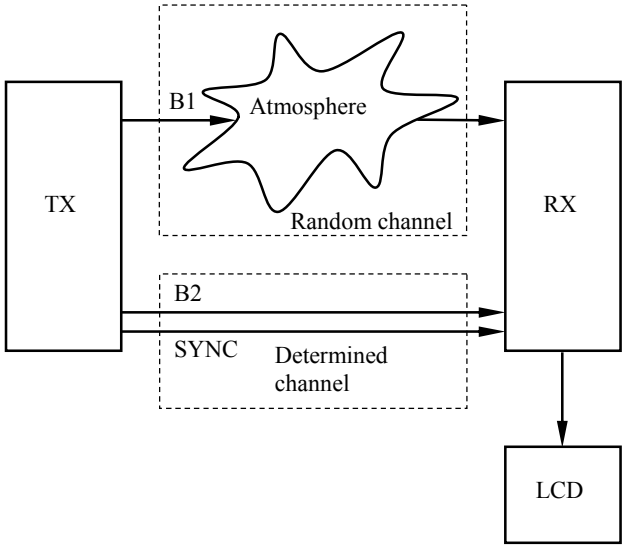

Fig. 2. Structure of BER calculating blocks

strong distortions through the atmosphere connection channel and there are also signals transmitted through a fixed-parameter channel. If the information has been transmitted without an error through the atmosphere channel, then at the output of the logical element in the receiver block at the moment of comparison there is a logical zero and there is no error aggregated. In the opposite case at the output of the logical element there is a logical one and respectively there is error aggregated. The results are visualized on a liquid crystal display.

The research stand of BER is based on microcontrollers PIC18F452. As the rest of the PIC microcontrollers, the microcontroller PIC18F452 uses HARVARD architecture, characteristic of which are the separate buses for access to the data memory and the programme memory Fig.3.

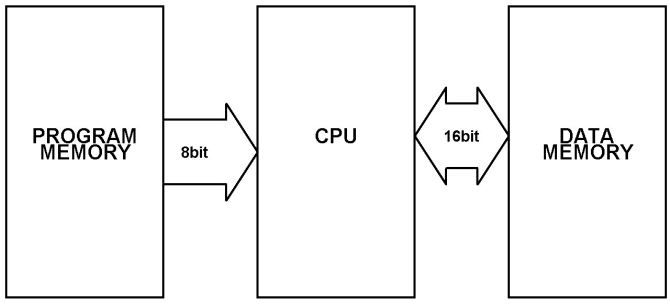

Fig. 3. Structure of chosen processor

The advantages of this are many but the most important is that the two buses can have different length (number of bits). This allows the 16-bit instructions of the microcontroller PIC18F452 to be extracted from a 16-bit data path for instructions, and the 8-bit data, respectively from an 8-bit data path. In these conditions the extracting and implementing of a 16-bit instruction takes one cycle, that is we have a greater productivity of the central processor.

The maximum clock frequency of the microcontroller PIC18F452 is 40 MHz. Before entering the central processor the clock signal is divided into 4 non-overlapping series which form an instruction cycle with a frequency of 10 MHz. Having in mind that the implementation of one instruction takes one cycle, when working with a maximum clock frequency, the productivity of the central processor will be 10MIPS (MIPS – million instructions per second). An exception to this are the transition instructions and the 32-bit instructions, the implementation of which takes two cycles.

A detailed description of the numerical part of the system as well as the consideration on the signal and subsystem level [15] is to be done in some of our further works.

IV. EXPERIMENTS

The initial check of the productivity of the system described in section III includes the power measurement of the receiver signal at random points and its comparison with the respective values calculated according to the theoretical model given in section II. The main experiments are two: check of the axial dependency of the optical field on the source within the distance of the test-bed; check of the radial dependency of the field by means of changing the azimuthally angle θ of the distribution direction of the beam.

For this purpose the receiver is replaced by a highly sensitive fiber-optic power meter with a low receiver aperture $A_r = 0{,}1mm^2$, sensitive within a wide wavelength interval, also including the central length of the optical radiation of the source $\lambda_0 = 850nm$.

The values of the parameters of the system at which the measurements are done and which are necessary for the numerical calculation, are: average optical source power $\Phi_L = 2mW\,(3dBm)$; angle divergence of the radiation after the transmitter antenna (the collimator) $\theta_t = 0{,}3rad$; distributed losses along the connection channel – $b_f = 0{,}1dB/km$ have been accepted, which is equals absolutely clean atmosphere ($S_M = 60km$).

The background optical radiation measured during the experiment by using measurements and wavelengths $1{,}31\mu m$ and $1{,}55\mu m$ (to increase the sensitivity and decrease the measurement error) is $\Phi_{r,B} = -69dBm$.

In Fig.4 we have shown the experimental (with dots) and theoretical (flat line) results for the change in the receiver power along the axis of the ray, that is the dependency $I(0,z)$, resp. $\Phi_r(0,z)$, for the distance between the transmitter and receiver $L \in [0{,}2m;1{,}7m]$ and for the movement of the ray away from the direction of the receiver antenna $\theta_t = 0$. There is a very good matching of the two results.

In Fig.5 we have presented the results from the comparison between the experimental and theoretical values for the

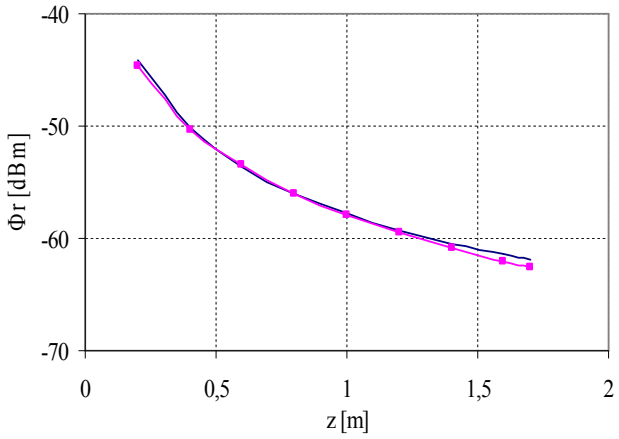

Fig. 4. Measured vs Calculated Data for Received Power

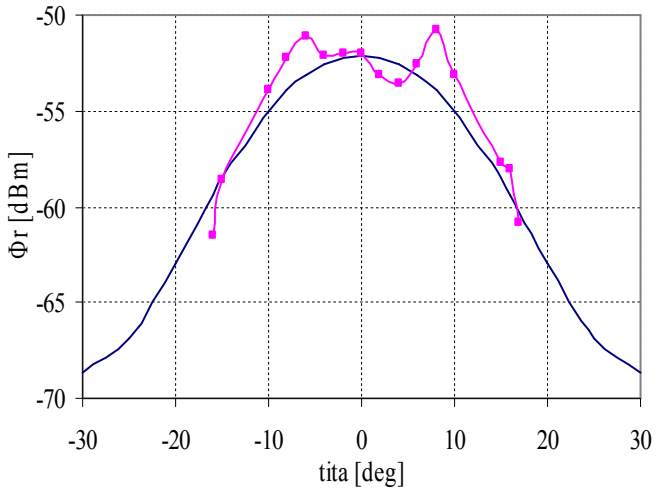

Fig. 5. Measured vs Calculated Data for axial Gaussian Distribution

checking of the axial Gaussian amplitude distribution of the optical radiation. The comparison has been conducted with $L = 0{,}5m$, $|\theta_t| \in [0;0{,}52rad]$, respectively $\rho \in [0;0{,}25m]$. The visible differences are mostly due to deviations in the amplitude distribution of the source of optical radiation from the ideal Gaussian one, which is observed with a great number of semiconductor sources, and even a very small azimuthally dependency of the background optical radiation $\Phi_{r,B}$, inevitable for the particular experimental setting.

V. Conclusion

We have conducted a theoretical analysis which has been verified by means of experimental results. This paper is part of a work which will include gradual detailed research on the FSO technology in laboratory and real environment.

References

[1] H. Willebrand, B. Ghuman, *Free Space Optics: Enabling Optical Connectivity in Today's Networks*, Indianapolis, SAMS, 2001.

[2] S. Hranilovic, *Wireless Optical Communication Systems*, Springer, 2004.

[3] S. Bloom, E. Korevaar,J. Schuster,H. Willebrand, "Understanding the performance of free-space optics", Optical Society of America, JON 2330 June 2003 / Vol. 2, No. 6 / JOURNAL OF OPTICAL NETWORKING, pp.178-200,2003.

[4] E. Ferdinandov, B. Pachedjieva, K. Dimitrov, *Optical Communication Systems*, Sofia, Technika, 2007.(in bulgarian)

[5] X. Zhu, J. M. Kahn, "Free-Space Optical Communication through Atmospheric Turbulence Channels", IEEE Trans. on Commun., vol. 50, no. 8, pp. 1293-1300, 2002.

[6] X. Zhu and J. M. Kahn, "Performance Bounds for Coded Free-Space Optical Communications through Atmospheric Turbulence Channels", IEEE Trans. on Commun., vol. 51, no. 8, pp.1233-1239, 2003.

[7] E Korevaar; I. Kim, B. McArthur, Atmospheric propagation characteristics of highest importance to commercial free space optics Proc. SPIE, Vol. 4976, Atmospheric Propagation, C. Young; J. Stryjewski, Editors, pp.1-12, 2003.

[8] A. Tunick, Optical turbulence parameters characterized via optical measurements over a 2.33 km free-space laser path, Optics Express, Vol. 16, Issue 19, pp.14645-14654, 2008.

[9] Al. Naboulsi1, M. Sizun H. de Fornel, "Propagation of optical and infrared waves in the atmosphere", XXVIIIth UNION RADIO-SCIENTIFIQUE INTERNATIONALE General Assembly, New Delhi, India, 2005.

[10] E. Ferdinandov, *Laser Radiation in Radiotechnique*, Sofia, Technika, 1981.(in bulgarian)

[11] X.Liu, Free-space optics optimization models for building sway and atmospheric interference using variable wavelength, IEEE Transactions on Communications, Vol.57, Issue: 2, pp.492-498, 2009.

[12] P. Corrigan, R. Martini, E. Whittaker, C. Bethea, Quantum cascade lasers and the Kruse model in free space optical communication, Optics Express, Vol. 17, Issue 6, pp. 4355-4359, 2009.

[13] K. Veselinov, F. Grillot, Al.Bekiarski, J. Even, S. Loualiche, "Numerical modelling of the two-state lasing in 1.55um (113)B InAs/InP quantum dot lasers for optical telecommunications", Sofia, ICEST, pp.260-261, 2006.

[14] K. Kazaura, K. Omae, T. Suzuki, M. Matsumoto, E. Mutafungwa, T. Korhonen, T. Murakami, K. Takahashi, H. Matsumoto, K. Wakamori, Y. Arimoto, Enhancing performance of next generation FSO communication systems using soft computing-based predictions, Optics Express, Vol. 14 Issue 12, pp.4958-4968, 2006.

[15] V. Georgieva, *Signals and Systems (laboratory manual)*, Sofia, Novi Znania, 2009.